



City Research Online

City, University of London Institutional Repository

Citation: Fu, F. (2022). Studies on CFST column to steel beam joints using endplates and long bolts under central column removal. *Steel and Composite Structures*, 42(2), pp. 161-172. doi: 10.12989/scs.2022.42.2.161

This is the accepted version of the paper.

This version of the publication may differ from the final published version.

Permanent repository link: <https://openaccess.city.ac.uk/id/eprint/28230/>

Link to published version: <https://doi.org/10.12989/scs.2022.42.2.161>

Copyright: City Research Online aims to make research outputs of City, University of London available to a wider audience. Copyright and Moral Rights remain with the author(s) and/or copyright holders. URLs from City Research Online may be freely distributed and linked to.

Reuse: Copies of full items can be used for personal research or study, educational, or not-for-profit purposes without prior permission or charge. Provided that the authors, title and full bibliographic details are credited, a hyperlink and/or URL is given for the original metadata page and the content is not changed in any way.

City Research Online:

<http://openaccess.city.ac.uk/>

publications@city.ac.uk

Studies on CFST column to steel beam joints using endplates and long bolts under central column removal

Shan Gao^{1,2,3}, Bo Yang³, Lanhui Guo², Man Xu^{4*} and Feng Fu⁵

¹ Shaanxi Key Laboratory of safety and durability of concrete structures, Xijing University, Xi'an, China

² School of Civil Engineering, Harbin Institute of Technology, Harbin, China

³ School of Civil Engineering, Chongqing University, Chongqing, China

⁴ School of Civil Engineering, Northeast Forestry University, Harbin, China

⁵ School of Mathematics, Computer Science & Engineering, University of London, London, U.K.

(Received keep as blank , Revised keep as blank , Accepted keep as blank)

Abstract. In this paper, four specimens of CFST column joints with endplates and long bolts are tested in the scenario of progressive collapse. Flush endplate and extended endplate are both adopted in this study. The experimental results show that increasing the thickness of the endplate could improve the behavior of the joint, but delay the mobilization of catenary action. The thickness of the endplate should not be relatively thick in comparison to the diameter of the bolts, otherwise catenary action would not be mobilized or work effectively. Effective bending deformation of the endplate could help the formation and development of catenary action in the joints. The performance of flexural action in the joint would affect the formation of catenary action in the joint. Extra middle-row bolts set at the endplates and structural components set below the bottom beam flange should be used to enhance the robustness of joints. A special weld access hole between beam and endplate should be adopted to mitigate the chain damage potential of welds. It is suggested that the structural components of joints should be independent of each other to enhance the robustness of joints. Based on the component method, a formula calculating the stiffness coefficient of preloaded long bolts was proposed whose results matched well with the experimental results.

Keywords: CFST; progressive collapse; endplate; catenary action; long bolts; component method

1. Introduction

The progressive collapse of structures has attracted much attention from civil engineers and building standard organizations (Mirtaheri 2016, Mashhadi 2017). In conventional design, the beam-to-column joints are designed to carry bending moment. However, when column loss happens, the vertical loads will be sustained by the beams connected to the damaged column (GSA 2003, DOD 2013). Catenary action is supposed to contribute to load resistance with the increasing of vertical displacement of the joint (Hoffman 2011, Khaloo 2018). In that case, an extra tensional force which is not considered in conventional design would exist in the joint and shows a remarkable influence on the mechanical performance of joint (Simos da Silva 2004). Especially, the ductility of the joints should meet the demand for the rotation ability to mobilize the catenary action in beams.

*Corresponding author, Associate Professor, E-mail: xuman@nefu.edu.cn

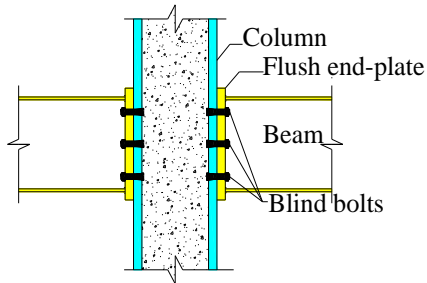


Fig. 1 Blind bolts

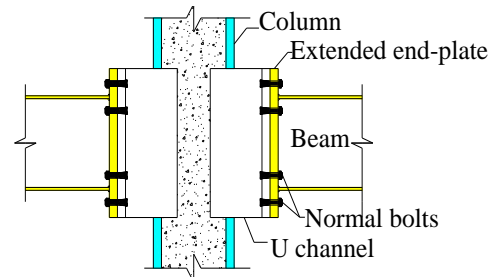


Fig. 2 U channel

In bolted concrete-filled steel tubular (CFST) joints, blind bolts or U channel could be adopted as shown in Fig. 1-2. These configurations could avoid the inconvenience of setting bolts inside the closed-section tube. However, these two configurations also have some disadvantages, such as high cost and relatively low bending performance which is determined by the wall of column or U channel. Even though some studies have been conducted on these joints (Hoang 2015, Elghazouli 2009), no design guidance is stipulated in current design codes.

In the past decades, many studies have been carried out on the behavior of steel beam to CFST-column joints. Li and Han (2011) conducted FE analysis to reveal the failure mode of steel-beam to CFST-column joints with RC slab. Thai and Uy (2012) proposed a model to calculate the bending resistance of endplate connections. Wang (2012) tested blind-bolted extended endplate CFST joints under bending moment whose rotation capacity could meet the requirements of the anti-seismic design. Huang et. al (2016) conducted an experimental study to validate against the proposed restoring force model for CFST joints. Tartaglia et. al (2018) discussed the influence of a wide range of parameters on the ultimate response of extended stiffened endplate joints through FE analysis.

Regarding the performance of joints in steel structures under column loss scenario, Izzuddin et. al (2008) proposed a method to evaluate the dynamic response of structures or joints under column loss. Démonceau and Jaspart (2010) studied the influence of catenary forces on the load-carrying performance of composite joints. Sadek et al. (2011) carried out experimental and numerical studies on the performance of bare steel connections in the scenario of column removal. Yang and Tan (2012) conducted a parametric analysis to reveal the influence of connection configuration on the anti-collapse behavior of joints. Stylianidis and Nethercot (2015) developed an approach to describe the performance of joints in anti-collapse analysis. Gao et. al (2017) concluded that the moment capacity of the joint decreases linearly with the increase of tensile load.

So far, the investigations conducted on steel beam to CFST column joint mostly employ the configuration of ring plates. In this paper, the endplate and long bolts are both used in the connections as shown in Fig. 3. By using long bolts, core concrete will anchor the bolts, while the tensile force in bolts would not be resisted by the wall of column directly, resulting in the improvement of the mechanical performance of the joint (Xu et. al 2018). Four specimens of CFST column joint with endplates and long bolts are tested in the scenario of middle column loss in this study. The failure modes and development of catenary action of the specimens are discussed in detail. Based on the experimental results, practical implications are suggested to improve the robustness of joints. A formula is developed to calculate the stiffness coefficient of preloaded long bolts for predicting the initial stiffness of the joints.

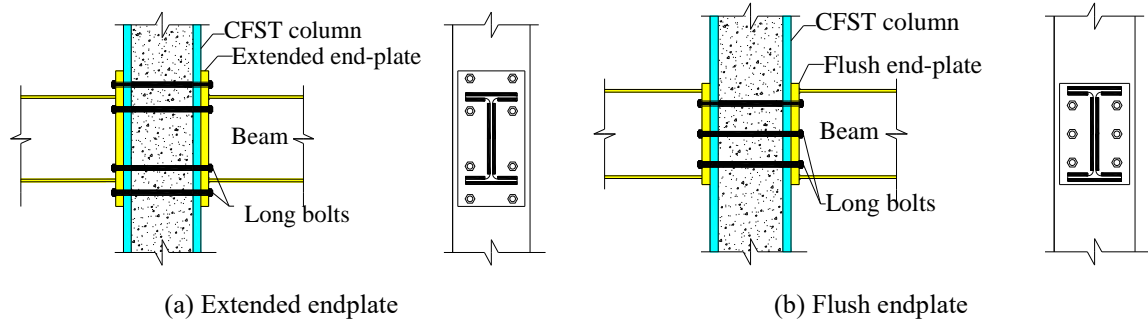


Fig. 3 Endplate joint with long bolts

2. Experimental program

2.1 Test specimen

The joint above the destructed column is extracted from a frame. Hinge supports are assumed at both ends of beams, since the inflection point locating at the middle span. The vertical loads would be applied at the top of the specimen in succession to study the anti-collapse behavior of the joint.

Four 2/3 scaled specimens were designed for the test, including two flush endplate connections and two extended endplate connections. The design of steel beams and CFST columns in the prototype structure were in accordance to GB50017-2017 (2017) for steel structures and GB50936-2014 (2014) for CFST structures respectively. The design of endplates and bolts in the connections was based on GB50017-2017 and EC 3 (2004). The design of the reduced scaled specimens is also based on the testing capacity of the equipment and the predicted failure mode of the connections. For instance, at least three rows of bolts should be placed in the flush endplate connection to make sure of the ductile failure. The number of bolts in an extended endplate connection should be similar to that in a flush endplate connection and cannot be too many to make its performance too similar to that of a rigid connection.

Fig. 4 and Fig. 5 show the overall dimensions of the specimens. High strength long bolts of Grade 10.9 were adopted to connect the endplate to CFST column. The dimensions of the endplate were shown in Fig. 6. 16 mm-diameter bolts were used for specimen FJ1, FJ2 and EJ1, while 20 mm-diameter bolts were for specimen EJ2. The thickness of endplate was 16 mm for specimen FJ1, EJ1 and EJ2, and 20 mm for specimen FJ2. The detailed dimensions of the specimens are summarized in Table 1. The pretension in Table 1 applied by using a mechanical torque wrench was derived from the design torsion based on GB50017-2017 (2017).

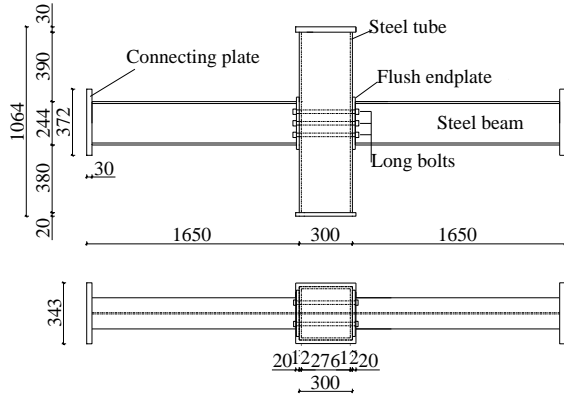


Fig. 4 Dimensions of flush endplate specimen(mm)

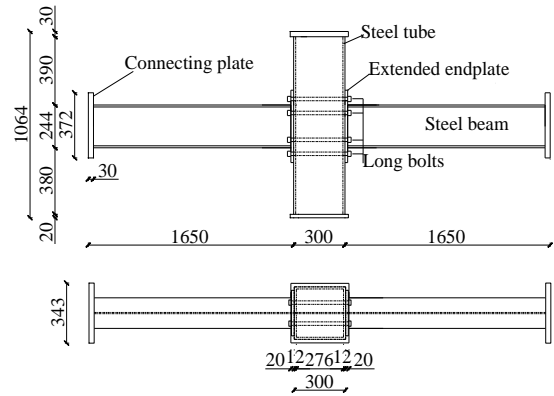


Fig. 5 Dimensions of extended endplate specimen (mm)

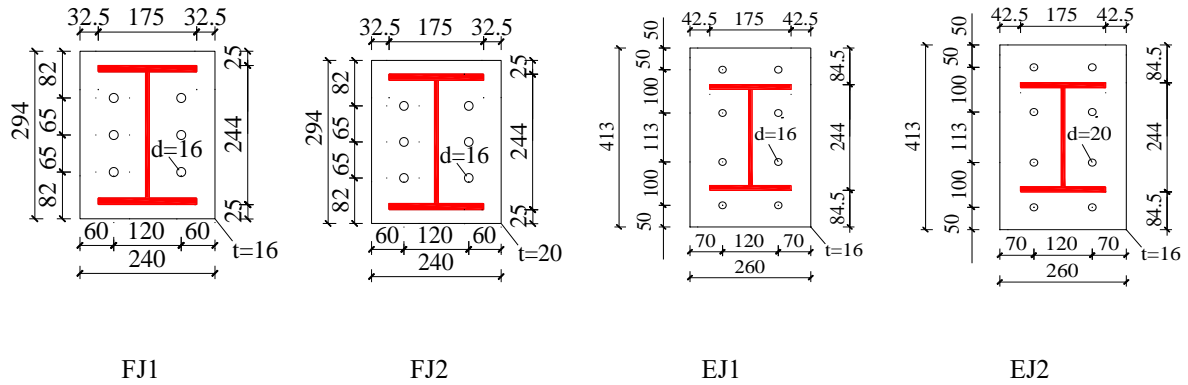


Fig. 6 Dimensions of endplates (mm)

Table 1 Parameters of specimens (mm)

Specimen ID	Steel members			Bolt diameter/mm	Pretension/kN
	Column	Beam	Endplate		
FJ1	□300×300×12	HM244×175×7×11	240×294×16	16	100
FJ2	□300×300×12	HM244×175×7×11	240×294×20	16	100
EJ1	□300×300×12	HM244×175×7×11	260×413×16	16	100
EJ2	□300×300×12	HM244×175×7×11	260×413×16	20	155

2.2 Material properties

The prisms for testing concrete strength and Young's modulus were cast and cured in the same lab with the specimens. The average compressive strength and Young's modulus of concrete were 40.6 MPa and 3.2×10^5 MPa respectively. The mechanical properties of the steel are listed in Table 2, where f_y , f_u , E_s stand for yield strength, tensile strength and Young's modulus of steel respectively. The mechanical properties of high strength bolts were provided by the supplier.

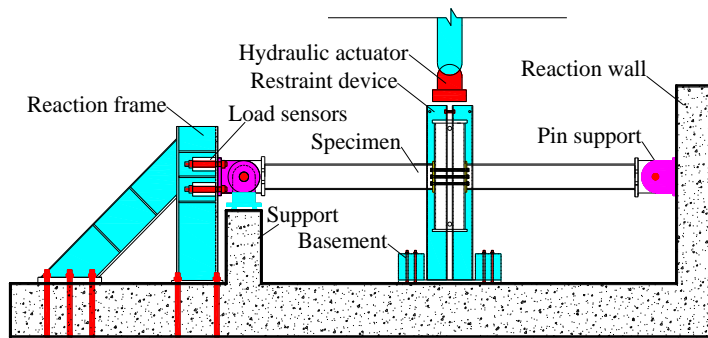
Table 2 Mechanical properties of steel

Se.	Grade	f_y (MPa)	f_u (MPa)	E_s (10^5 MPa)
Beam	Flange	333.81	464.03	2.04
	Web	321.47	467.16	2.03
Endplate	16 mm	362.26	468.94	2.01
	20 mm	353.44	461.73	2.03
Tube wall		380.89	490.23	2.05
Bolt	10.9	1089.00	1210.00	2.06

2.3 Experimental setup

As shown in Fig. 7, a combination of reaction frame and reaction wall provided the horizontal restraint for the specimens. A restraint device was installed to restrain the out-plane displacement and rotation of the specimens. The axial force in the beams was recorded by the horizontal load sensors. Extra vertical support was set under the pin support to accommodate the shear force on the screws connecting the load sensors to the reaction frame. A displacement-control loading procedure was adopted by a hydraulic actuator at a rate of 6 mm/min.

The vertical displacement of beams and the horizontal displacement of a column in specimens were recorded by linear variable displacement transducers (LVDTs) as shown in Fig. 8 (a). Strain gauges were placed on two sections of both sides of the steel beams as shown in Fig. 8 (b). The internal forces in beams could be estimated based on the data from strain gauges and compared with the data from horizontal load sensors.



(a) Elevation view



(b) Out-plane restraint device

Fig. 7 Experimental setup

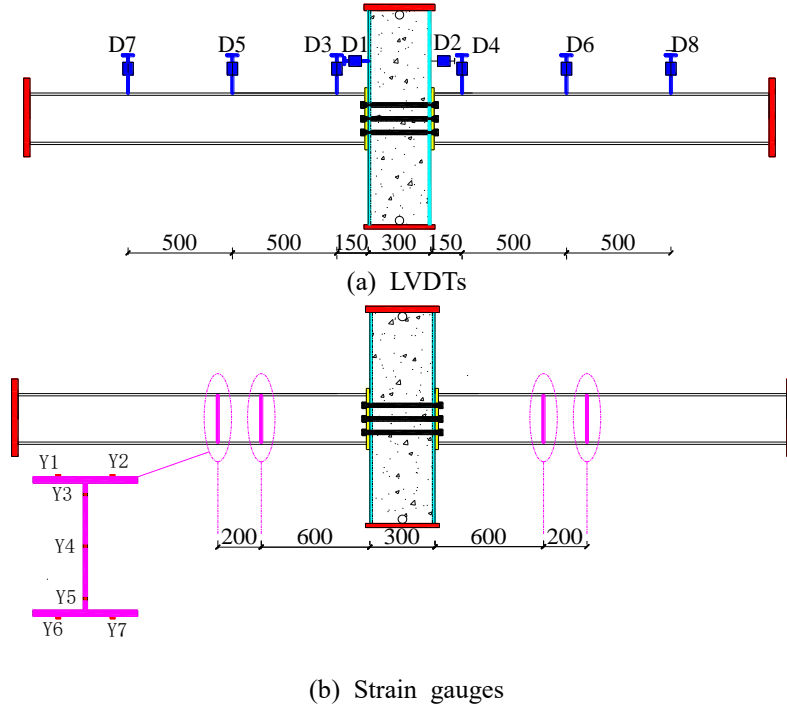


Fig. 8 Distribution of measuring equipment

3. Experimental results and discussions

After middle column removal, the total vertical load P carried by the joint is composed of the load carried by flexural action (P_{fa}) and the load carried by catenary action (P_{ca}):

$$P = P_{fa} + P_{ca} \quad (1)$$

The load P_{ca} could be described by axial force N_a in beams and the joint rotation α in Eq. (2):

$$P_{ca} = 2N_a \sin \alpha \quad (2)$$

The axial force N_a could be obtained from the horizontal load sensors as shown in Fig. 7, or from the strain of beam section obtained from the strain gauge as shown in Fig. 8(b) which could be described by Eq. (3):

$$N_a = E_s A_b \left(\sum_{i=1}^n \varepsilon_i \right) / n \quad (3)$$

where E_s is Young's modulus of steel, A_b is the beam area and ε_i is the strain data obtained from the i th strain gauge at the beam section.

3.1 Flush endplate joints

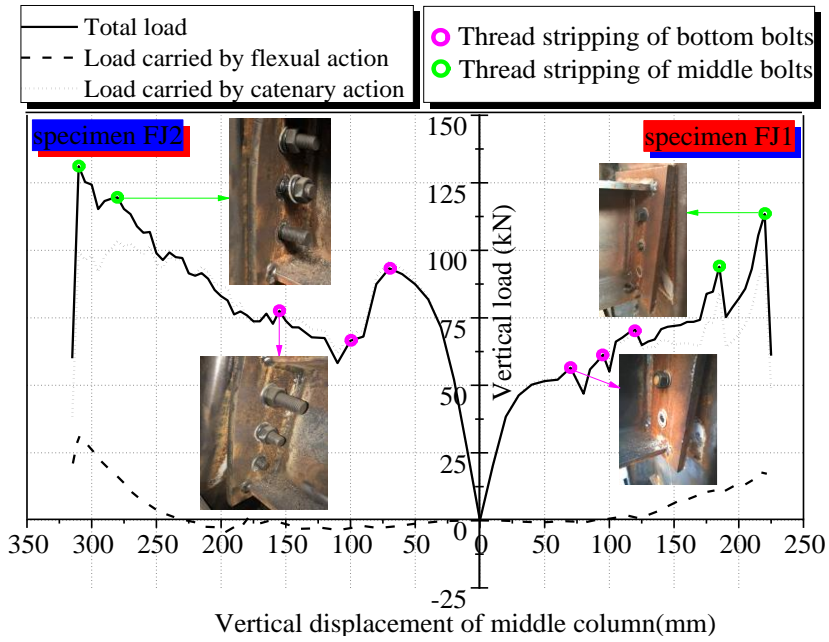
16-mm thickness flush endplate and 16-mm diameter bolts were used in specimen FJ1. Fig. 9(a) shows the vertical load v.s. middle column displacement curves of specimen FJ1. The curves representing the loads carried by flexural action and catenary action were calculated by Eq. (1-3). It indicated that the vertical load on specimen FJ1 was carried by flexural action in the initial stage.

Along with the increase of vertical displacement, the curve developed into a hardening stage of flexural action where catenary action was still not triggered. In this stage, thread stripping of bottom bolts happened which brought about three slumps. After thread stripping occurred in all four bottom bolts at the displacement of 125 mm, catenary action began to contribute to the load-carrying. Subsequently, total load began to exceed the load carried by flexural action and more thread stripping of bolts also occurred in succession. It was worth noticing that catenary action only afforded 17 percent of the total load before the joint failed which meant that the transition from flexural action to catenary action was insufficient in specimen FJ1. The test was terminated by the thread stripping of all four bolts in the middle row. A slight buckling was also observed at the right side of the top beam flange as shown in Fig. 10 (a).

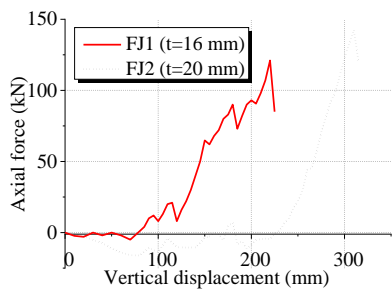
20-mm thickness flush endplate and 16-mm diameter bolts were used in specimen FJ2. The vertical load on specimen FJ2 was initially carried solely by flexural action as illustrated by the comparison of three curves in Fig. 9(a). Thread stripping of bottom bolts at the right side of connection occurred which resulted in a sharp slump at the curves. After then, thread stripping of bottom bolts at the left side of the connection happened two times successively which prevented the load increased significantly. After four bottom bolts all failed, the vertical load began to increase steadily until thread stripping of middle bolts occurred at the displacement of 295 mm. Fig. 9(a) also indicates that catenary action was mobilized at the displacement of 230 mm. After then, the load carried by bending action almost stopped rising. Before the joint failed at 310 mm, catenary action carried 24 percent of the total load. Three out of four middle bolts were stripped at the displacement of 310 mm where the test was terminated. Compressive flange buckling was observed at both sides of the joint as shown in Fig. 10 (b).

It should be mentioned that not all middle bolts in the connections failed at this stage. If the loading procedure was continued, the vertical load can be further increased until all bolts in the middle and top rows failed, based on the results in Yang (2012) and Li (2011). The test was terminated due to the consideration of safety and limitation of the experimental setup.

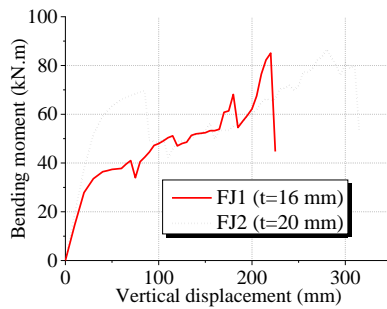
Fig. 9 also show the comparison of two specimens with different thickness of flush endplate ($t=16$ mm and 20 mm). The initial stiffness, yield load capacity, deformation capacity and maximum load capacity of the joint were all improved significantly by increasing the thickness of the endplate. Fig. 9(b) indicates that increasing the thickness of the endplate would increase the bending resistance of the joint and delay the mobilization of catenary action which explains the overlap portion of the curves from 100 mm to 200 mm in Fig. 9 (a). From Fig. 9 (c), it could be seen that the maximum flexural action was not increased, due to the limitation of bolts. As shown in Fig. 9(d), the bending moment did not decrease with the increase of axial force.



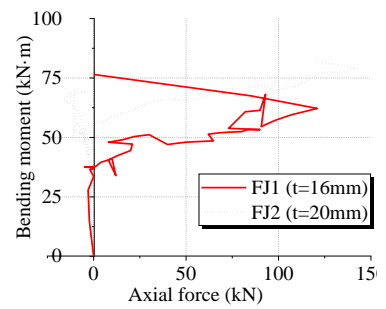
(a) Vertical load–middle column displacement curve



(b) Axial force of left beam–vertical displacement curve



(c) Moment of left connection–vertical displacement curve



(d) Moment–axial force relationship curve

Fig. 9 Comparison of specimens FJ1 and FJ2

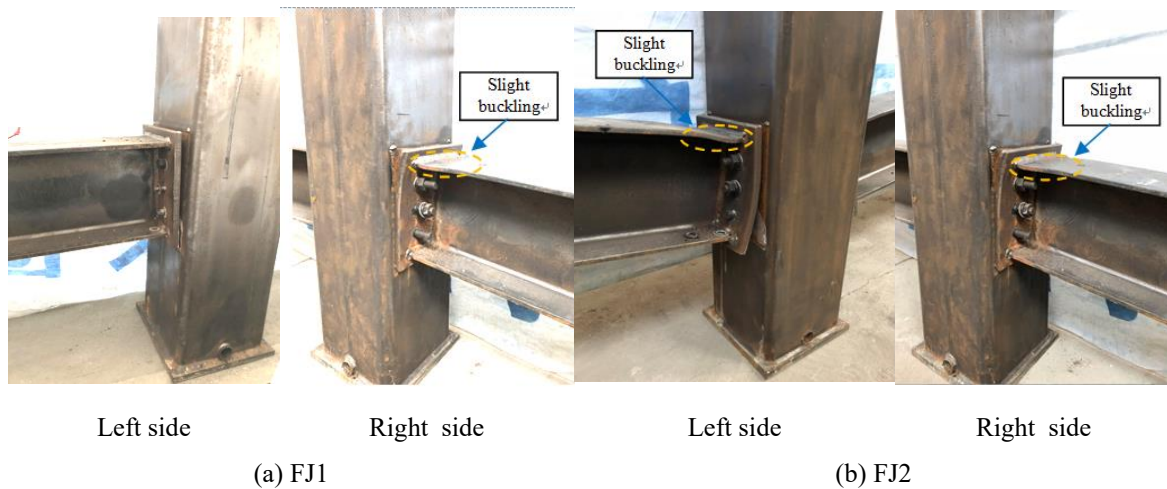


Fig. 10 Flush endplate specimens after tested

3.2 Extended endplate joints

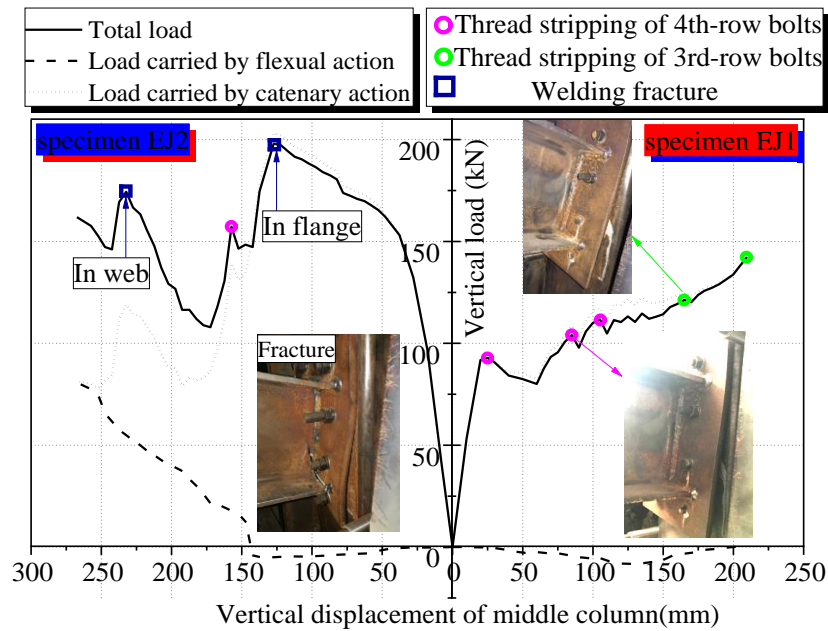
16-mm thickness extended endplate and 16-mm diameter bolts were used in specimen EJ1. The bolts above the top flange of steel beam were defined as the 1st-row which made the bolts below the bottom flange of steel beam the 4th-row, so as the bolts in specimen EJ2.

Fig. 11(a) shows the vertical load v.s. middle column displacement curves of specimen EJ1. When the vertical displacement increased to 25 mm (the corresponding load was 92 kN), the vertical load began to decrease slowly which indicated that thread stripping of 4th-row bolts was triggered. When the vertical displacement reached 60 mm, the vertical load began to increase again. After then, with the increase of vertical displacement, thread stripping occurred again until all 4th-row bolts had failed. Every time the thread stripping happened, a drop was observed in the curves. When the vertical displacement increased to 175 mm, thread stripping of bolt occurred in the 3rd row of the left side of the joint. All left side 3rd-row bolts of the joint had failed, when the vertical displacement reached 210 mm. Right then, the left side deformation of the joint was much larger than the right side. The test was terminated due to the consideration of safety.

Meanwhile, as shown in Fig. 11(a), no catenary action was triggered during the whole loading procedure. All vertical loads were resisted by flexural action. Due to the compressive strain in the beams and the adoption of the calculation method in Eq. (1-3), the load carried by flexural action was even larger than the total load applied which was no practical meaning. This phenomenon may be explained by two reasons: (1) the endplate was too thick, so that the vertical deformation of the joint was too small to trigger catenary action. (2) Four rows of bolts were set around the top and bottom flange of steel beam. No row of bolts was arranged in the middle of the endplate. After two rows of bolts around the bottom flange had failed, the remaining two rows of bolts were located around the compressive center which made the joint hardly carry the vertical load anymore.

The failed specimen was shown in Fig. 12. It was worth noticing that the shape of endplate was still a polygonal line after the all 3rd-row and 4th-row bolts of the left side in the joint failed, as shown in Fig. 12 (a). The rotation center or the compressive center of the connection is located at the compressive top flange of steel beam. The deformation shape of endplate indicated that the

thickness of endplate may be too thick in the design, compared with the bolt diameter.



(a) Vertical load–middle column displacement curve

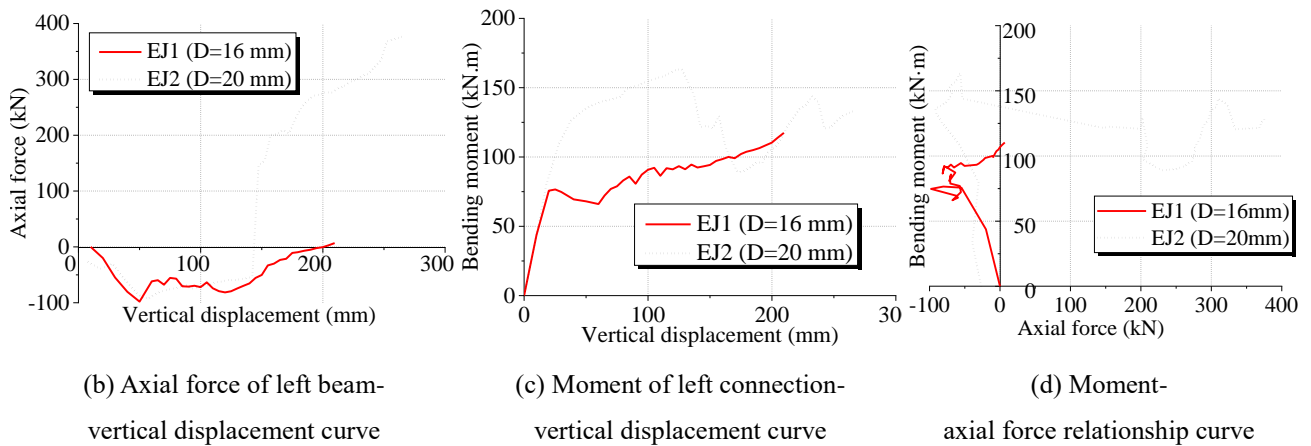


Fig. 11 Comparison of specimens EJ1 and EJ2

16-mm thickness extended endplate and 20-mm diameter bolts were adopted in specimen EJ2. The weld between the bottom flange and endplate of the left side of the joint fractured as shown in Fig. 11 (a) when the vertical displacement reached 125 mm. The fracture caused a sharp drop in the curves. Partial thread stripping of 4th-row bolts happening at the left side of the joint prevented the rising of vertical load at the displacement of 150 mm. From 170 mm, the vertical load began to increase along with the increase of vertical displacement. The weld between beam web and endplate of the left side of the joint fractured at 230 mm which cause a drop in the curves. The beam web was torn up successively. The shape of the endplate after the test exhibited a curve line.

As shown in Fig. 11(a), catenary action was mobilized at about 150 mm where partial thread stripping occurred at the 4th row of bolts. It is worth noticing that even the total load and the load carried by flexural action both decreased at 230 mm due to the fracture of wed weld, the load carried by catenary action kept rising. Before the joint failed at 270 mm, catenary action carried 50 percent of the total load. The test was terminated at 270 mm, due to the consideration of safety. The failed specimen was shown in Fig. 12 (b).

Fig. 11 also shows the comparison of two extended endplate specimens with different diameter bolts ($D=16$ mm and 20 mm). The diameter of bolts had a significant influence on the load capacity of the extended endplate joint. Even though the maximum vertical displacement of specimen EJ2 was larger than that of specimen EJ1, the vertical displacement corresponding to the maximum load of specimen EJ2 was smaller than that of specimen EJ1. Fig. 11 (b) shows that catenary action was triggered by increasing bolt diameter which also proves that the endplate in specimen EJ1 was too thick, compared with bolt diameter. From Fig. 11 (c), it could be seen that the maximum flexural action was increased by using larger diameter bolts. As shown in Fig. 11(d), the bending moment of specimen EJ2 decreased with the increase of axial force, whilst that of specimen EJ1 did not, since the axial force in specimen EJ1 was at a rather low level.

As shown in Fig. 12(a), the deformation mode of specimen EJ1 was similar to that of flush endplate joint. If the endplate is thick enough, the tensile force in the bottom bolts would make the endplate rotate around the top flange of beam. If the endplate is not thick enough, bending deformation would occur near the bottom flange of the beam as shown in Fig. 12 (b). It is obvious that the deformation mode of specimen EJ2 was more advantageous than that of specimen EJ1, due to its ductile behavior.



Failed specimen



Endplate deformation

(a) EJ1



Failed specimen

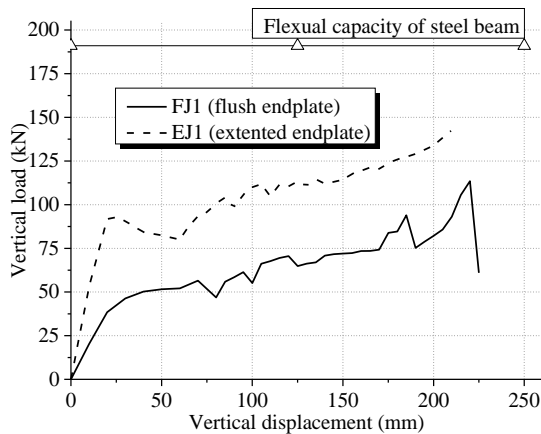
Endplate deformation

(b) EJ2

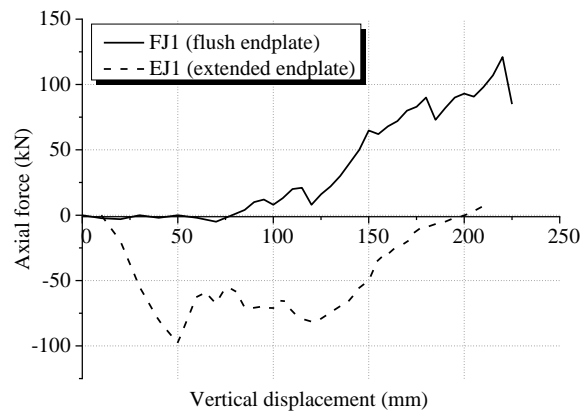
Fig. 12 Extended endplate specimens after test

3.3 3.3. Comparison of Specimen FJ1 and EJ1

Fig. 13 shows the comparison of specimen FJ1 with flush endplate and specimen EJ1 with extended endplate. The thickness of the endplate and diameter of bolts in these two specimens were both identical. Fig. 13 (a) implies that the configuration of the extended endplate would improve the behavior of joint, except for maximum vertical displacement. As described above, the deformation mode of endplate in specimen EJ1 was similar to that in specimen FJ1, due to the large thickness. In that case, the maximum vertical displacement would depend on the behavior of bolts, which made specimen FJ1 and specimen EJ1 have a similar deformation capacity. Due to the use of more bolts and better arrangement of bolts for bending moment, the load carried by flexural action and total load in specimen EJ1 were still larger than those in specimen FJ1, even catenary action totally was not mobilized in specimen EJ1.



(a) Vertical load–middle column displacement curve



(b) Axial force of left beam–vertical displacement

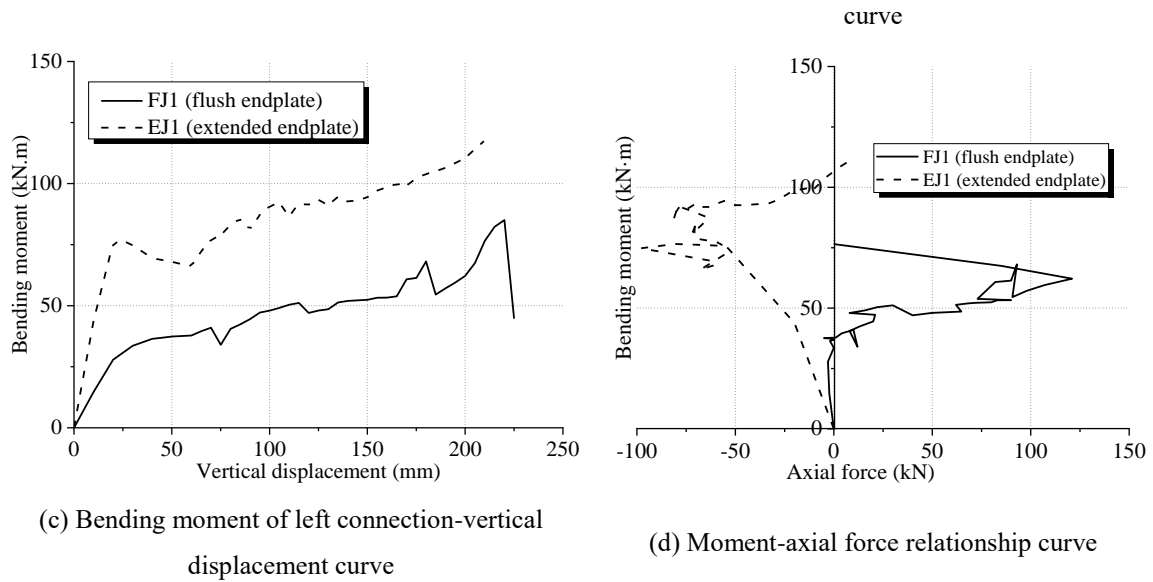


Fig. 13 Comparison of specimens FJ1 and EJ1

4. Discussions

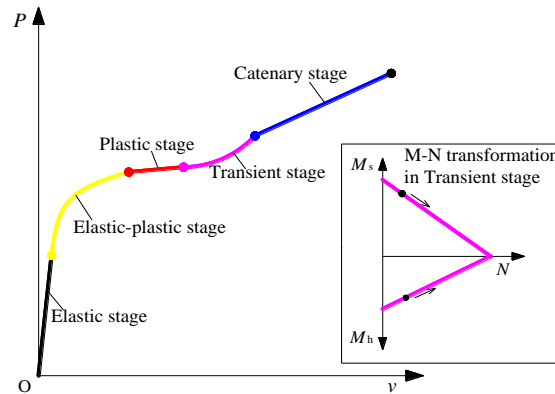
4.1 Influence of catenary action

Table 3 lists the comparison of the load capacity with and without considering catenary action. Generally, catenary action would improve the anti-collapse capacity of the flush endplate specimens by 20% and 27% respectively. Increasing the thickness of the flush endplate would help catenary action to carry more loads. In contrast, catenary action does not influence the load capacity of the extended endplate specimens, even the catenary action in specimen EJ2 has carried 50 percent of the load before the joint failed. These results imply that the thickness of the endplate should match the diameter of bolts, otherwise catenary action would not be mobilized or work effectively. Effective bending deformation of endplate could help the formation and development of the catenary action in the joints.

As described in Gao (2017), the development of load-carrying mechanism of joints could be divided into elastic stage, elastic-plastic stage, plastic stage, transient stage and catenary stage. The moment-tensile force relationship of joints is supposed to be linear and the strengthening of load-carrying capacity is not considered as shown in Fig. 14.

In this study, except for specimen EJ1, the other three specimens are all in the transient stage where flexural action and catenary action carry loads together. By increasing the thickness of the endplate, the elastic-plastic stage of specimen EJ2 is prolonged which would delay the transient stage. From the results of specimen EJ1, after flexural action is weakened by thread stripping, catenary action is triggered. It implies that specimen EJ1 is forced to go into the transient stage. Based on the discussion and comparison of experimental results, it could be concluded that the flexural action of joint would affect the formation and development of catenary action. The more loads the flexural action of joint could carry, the later the catenary action of joint forms. However,

the weakening of flexural action would force the formation of catenary action in joint.



Note: M_s is the sagging moment resistance; M_h is hogging moment resistance

Fig. 14 Progressive collapse behavior of the sub-structure

Table 3 Comparison with and without catenary action

Specimen ID	Load capacity with catenary action/kN	Load capacity without catenary action/kN	Load capacity increase due to catenary action /%	Percentage of load carried by catenary action before joint failed /%	Failure mode
FJ1	113	94	20	17	Bolt thread stripping
FJ2	131	103	27	24	Bolt thread stripping
EJ1	142	142	0	0	Bolt thread stripping
EJ2	198	198	0	50	Weld fractured & partial thread stripping

4.5 Practical implication of the experimental results

According to the failure modes of four specimens, it should be noticed that bolt thread stripping is not a reasonable failure mode of joints, due to its unpredictability, just like the fracture of welds between bottom flange and endplate. The failure mode of joints should be predictable in practical design, such as fracture of bolts or buckling of beam flange. However, the failure mode of bolt thread stripping also occurred in similar tests of Yang (2012). In Yang (2012), seven types of bolted joints were tested in the scenario of middle column removal where the failure mode of thread stripping was only observed in endplate joints. Compared to the connection configuration in this study, 20 mm-diameter bolts and 12 mm-thickness endplate were used in the specimens of Yang (2012) which indicated that the bolts were supposed to be strong enough in the connections.

Based on the experimental phenomena in this study and Yang (2012), it may indicate that the configuration of endplate was vulnerable to this unpredictable premature failure as shown in Fig. 15. Double nuts may be used in the configuration of endplate joints to avoid the unpredictable failure mode of thread stripping. More studies should be done on this issue in the future.

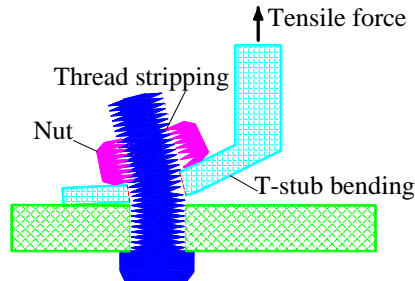


Fig. 15 Thread stripping in T-stub

In robustness design, the structure system should have the capacity to redistribute the additional loads to adjacent structural members in the scenario of single, even multiple structural member loss, namely alternative path method in GSA (2003). From a similar perspective, beam-to-column joints should also possess the ability to maintain the load-carrying in the loss of connecting components. Although the structural components in bolted endplate joint include beams, column, bolts and endplates, the reason causing the failure of the joint in most cases is the failure of bolts (fracture, thread stripping or pulled out of bolt hole) or the fracture welds between endplate and beam. Hence, the robustness assessment models for the specimens in this test could be assembled as shown in Fig. 16.

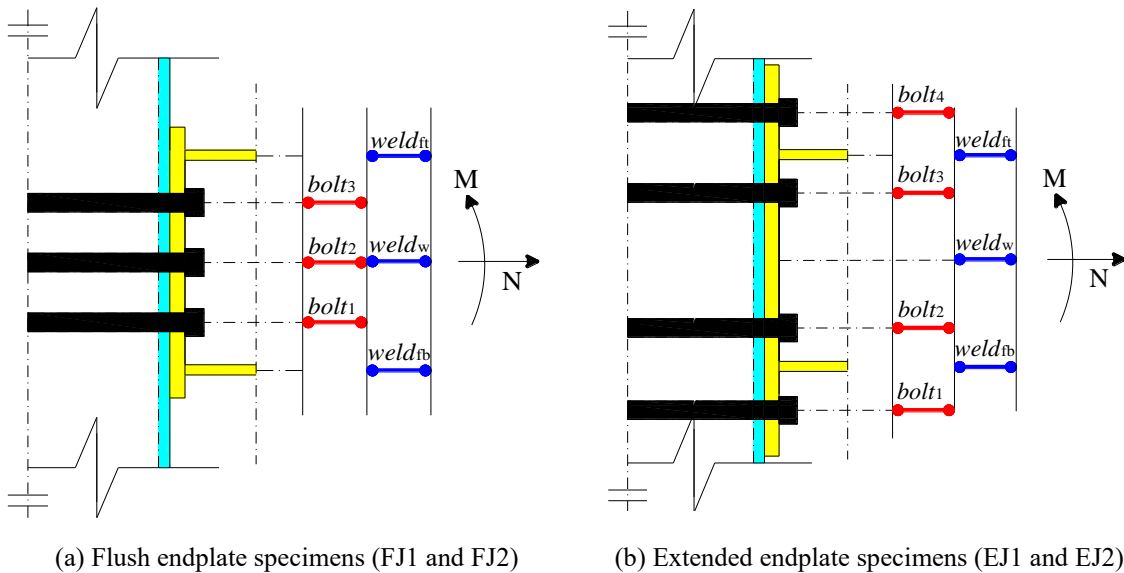


Fig. 16 Robustness assessment models

For both flush endplate and extended endplate specimens, the failure of bolt1 would result in a drop of moment resistance, whilst the failure of bolt2 would cause the failure of the joints. It indicates that the bolt2 redistributes the additional loads which are caused by the failure of bolt1.

On the contrary, the bolt3 and the bolt4 set in the extended endplate joint have little influence on the robustness of joints under sagging moment and tensional force. Although it is well known that the bolts should be installed near beam flanges to carry bending moment, extra bolts are suggested to be set midway at the endplates to enhance the robustness of joints. Besides, in the scenario of pure tensile force, the bolts set midway at the endplates behave better than the bolts near beam flanges, due to the little deformation of the middle portion of endplate under tension.

According to the experimental phenomena in this test and Gao (2017), the failure of weldfb (connecting endplate and bottom beam flange) would easily lead to the failure of weldw (connecting endplate and beam web), and then cause the failure of the joint. To avoid the premature failure of beam section, the extra components should be set below beam bottom flange, such as bottom cover plate, middle stiffener and bottom haunch suggested in DoD (2013).

Moreover, the chain damage potential of weldft and weldw should be mitigated. To this end, the configuration of weld access hole could be adopted in endplate. Commonly, this configuration is used in the rigid joints between bottom beam flange and column flange, rather than in endplate joints (Hoang 2015). The details of the weld access hole provided in FEMA-350 (2000) for the connection between beam flange and column flange as shown in Fig. 17 may also be used in endplate joints between beam and endplate. Besides minimizing stress and strain concentration, the chain damage potential of weldft and weldw may be mitigated by using this configuration. It also implies that, to enhance the robustness of joints, the structural components of joints should be independent of each other.

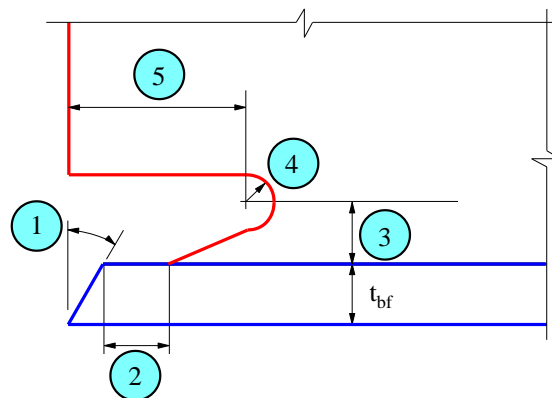


Fig. 17 Weld access hole (FEMA350 2000)

5. Analysis using component method

The component method is recommended in Eurocode 3 (2005) to predict the behavior of steel joints. By using this method, steel joints are decomposed into a series of structural components under various internal forces, such as endplate in bending and flange in compression. The stiffness and load capacity of these components are calculated successively. Finally, the assembly of these structural components could present the behavior of joints under various loading scenarios.

The structural components for the specimens under flexural action in this study include: bolts in tension (bt), beam flange in tension and compression (bft, bfc), beam web in tension and compression (bwt and bwc), endplate in bending (eb) and column in compression (cc). No shear

failure of bolts was observed in this test, therefore the component of bolts in shear is not considered in the model. After catenary action is triggered in the beams, the components of beam flange and web in compression would gradually transfer to those in tension whilst column in compression would cease to act anymore.

The components mentioned above are basic components covered in Eurocode 3 (2005). The design method proposed by Eurocode 3 could be used directly. It should be mentioned that the bolt preloading effect is not considered in Eurocode 3. The stiffness and capacity of column in compression could be taken as equal to infinity, due to the presence of in-filled concrete and symmetry of loading condition (2016). If not, a design method proposed for H-shape column encased in concrete by Eurocode 4 (2005) could be used to calculate the stiffness and capacity of column in compression.

Fig. 18 shows the component model of flush endplate specimen and extended endplate specimen. To simplify the calculation process, the components located in the same row would be assembled into one equivalent spring. It should be mentioned that, if tensile force is large enough, there would be no compressive area in the joint which meant the compressive components in the first row in Fig. 16 would be transferred to tensile components in the bottom row.

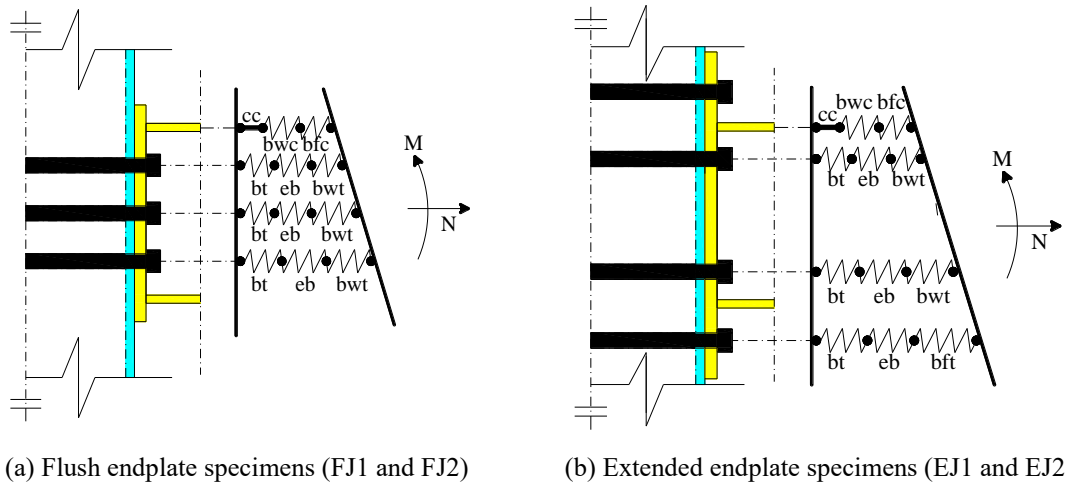


Fig. 18 Component models

Based on the component model in Fig. 16, the initial stiffness S_{ini} of joints could be determined from Eq. (4) in Eurocode 3 (2005):

$$S_{ini} = \frac{E_s z_{eq}^2}{\sum_i \frac{1}{k_i}} \quad (4)$$

where E_s stands for Young's modulus of steel; z_{eq} for the equivalent lever arm; k_i for the stiffness coefficient for component i .

For beam flange in tension and compression (bft, bfc) and beam web in tension and compression (bwt and bwc), the stiffness coefficient should be taken as equal to infinity (2005). For endplate in bending (eb), the stiffness coefficient k_{eb} could be determined by Eq. (5) in Eurocode 3:

$$k_{eb} = 0.9 I_{eff} t_{eb}^3 / m^3 \quad (5)$$

where l_{eff} stands for the smallest of the effective lengths given in Eurocode 3 (2005); t_{ed} for the thickness of endplate; m for the distance of bolt-hole center to beam web.

Referring to bolts in tension (bt), k_{bt} is obtained by Eq.(6):

$$k_{bt} = 2c_p A_b / L_b \quad (6)$$

where A_b is the effective tensile area of bolt; L_b is the bolt elongation length, taken as equal to the grip length (total thickness of material and washers), plus half the sum of the height of the bolt head and nut. The coefficient c_p is 0.8 if considering the effect of prying force and 1.0 if prying force is not triggered or taken into account, respectively.

The bolt preloading effect which plays an important role in the rotation stiffness of joint is not considered in Eq. (6). If bolt preloading is ignored in this test, the coefficient k_{bt} for bolts in tension would be very small, since long bolts are used in the joints which would cause a large value of bolt elongation length L_b . Based on the expression in Faella (1998), Eq. (7) is proposed to determine the stiffness coefficient of preloaded long bolts used in this study:

$$k_{bt} = 2c_p (4.10 + 3.25 \frac{B_c + 2t_{ed}}{d_b}) \frac{A_b}{L_b} \quad (7)$$

where B_c stands for the width of column; t_{ed} for the thickness of endplate; d_b for the diameter of long bolt.

The stiffness coefficient for the components and the assembly procedure to compute the initial stiffness of joint are shown in Table 4. As Table 4 shows, good agreements are obtained between test results and component-model results, especially for the extended endplate specimens. In addition, the stiffness coefficient of bolts in tension without considering the preloading effect is also provided which shows a large difference with the value obtained from Eq. (7). More studies still need to be conducted on the stiffness coefficient of preloaded long bolts.

Table 5 Component assembling for initial stiffness

	FJ1	FJ2	EJ1	EJ2
Stiffness	∞	∞	∞	∞
coefficient/mm				
$k_{bft}/k_{bfc}/k_{bwt}/k_{bwc}$				
$k_{cb,i}(\text{row1/row2/row3})$	8.4/8.4/8.4	16.8/16.4/16.4	24.9/8.4/8.4	24.9/8.4/8.4
k_{bt}	61.1(0.71*)	60.4(0.70*)	62.0(0.72*)	76.7(1.10*)
Lever arm $z_i(\text{row1/row2/row3})/\text{mm}$	181.5/116.5/51.5	181.5/116.5/51.5	273/173/60	273/173/60
Effective stiffness coefficient for each bolt				
row				
(row1/row2/row3)/mm	7.4/7.4/7.4	12.9/12.9/12.9	17.7/7.4/7.4	18.8/7.6/7.6
$k_{eff,i} = (\frac{1}{k_{cb,i}} + \frac{1}{k_{bt}})^{-1}$				
Effective lever arm/mm				
$z_{eq} = \frac{\sum_i k_{eff,i} z_i^2}{\sum_i k_{eff,i} z_i}$	140.7	140.7	239.1	240.0
Effective stiffness coefficient/mm				
$k_{eq} = \frac{\sum_i k_{eff,i} z_i}{z_{eq}}$	18.3	32.1	27.5	28.7
Initial stiffness of joint (model)/kNm/rad	74790	130687	323732	340770

$$S_{mi} = \frac{E_s z_{eq}^2}{1/k_{eq}}$$

Test initial stiffness/kNm/rad	85668	112969	337641	362038
--------------------------------	-------	--------	--------	--------

(*) means the value calculated using Eq. (6) which is not considering bolt preloading effect

6. Conclusions

This paper presents an experimental and analytical investigation of CFST column joint using endplates and long bolts under the middle column loss scenario. The experimental phenomena and results are discussed in detail. The following conclusions are made:

1). The configuration of endplate may be vulnerable to thread stripping failure. Double nuts should be used in the configuration of endplate joints to avoid unpredictable failure.

2). Increasing the thickness of endplate could improve the behavior of the joint, but delay the mobilization of catenary action. The diameter of bolts had a significant influence on load capacity of extended endplate joint and the formation of catenary action. The configuration of extended endplate would improve the behavior of joint, even when catenary action was not mobilized.

3). The thickness of endplate should not be relatively thick in comparison to the diameter of bolts, otherwise catenary action would not be mobilized or work effectively. Effective bending deformation of endplate could help the formation and development of catenary action in the joints.

4). The performance of flexural action in joint would affect the formation of catenary action in joint. The more loads the flexural action of joint could carry, the later the catenary action of joint forms. The weakening of flexural action would force the formation of catenary action in joint.

5). Extra middle-row bolts set at endplates and structural components set below the bottom beam flange could enhance the robustness of joints. A special weld access hole between beam and endplate should be adopted to mitigate the chain damage potential of welds which implies that the structural components of joints should be independent with each other to enhance the robustness of joints.

6). Based on the component method, a formula calculating the stiffness coefficient of preloaded long bolts was proposed, whose results matched well with the experimental results.

Acknowledgments

The project is supported by National Natural Science Foundation of China (NO. 51908085), Natural Science Foundation of Chongqing (cstc2020jcyj-msxmX0010), Fundamental Research Funds for the Central Universities (2020CDJ-LHZZ-013), and the Youth Innovation Team of Shaanxi Universities (21JP138) which are gratefully acknowledged.

References

- Demonceau J.F. and Jaspart J.P. (2010), "Experimental test simulating a column loss in a composite frame", *Advanced Steel Construction*, **6**:891-913.
- Department of Defense U.S. (2013), "Unified Facilities Criteria: Design of Building to Resist Progressive Collapse", UFC 4-023-03, USA.

- EN1993-1-8, European Committee for Standardization – CEN (2005), Eurocode 3: design of steel structures. Part 1.8, Design of joints, Brussels.
- EN 1994-1-1, European Committee for Standardization – CEN (2005), Eurocode 4: design of composite steel and concrete structures. Part 1.1, General rules and rules for buildings, Brussels.
- Elghazouli A.Y., Mágala-Chuquitaype C., Castro J.M. and Orton A.H.(2009), “Experimental monotonic and cyclic behavior of blind-bolted angle connections”, *Engineering Structures*, **31**: 2540–2553.
- Federal Emergency Management Agency (2000), “FEMA-350: Recommended Seismic Design Criteria for New Steel Moment-Frame Buildings”, USA.
- Faella C., Piluso V. and Rizzano G. (1998), “Experimental analysis of bolted connections: snug versus preloaded bolts”, *Journal of Structural Engineering*, **124**: 764-744.
- Gao S., Guo., Fu F. and Zhang S.M. (2017), “Capacity of semi-rigid composite joints in accommodating column loss”, *J. Constr. Steel Res.*, **139**: 288-301.
- GB50017-2017 (2017). Code for design of steel structures. Beijing, China.
- GB50936-2014 (2014). Technical code for concrete filled steel tubular structures. Beijing, China.
- General Services Administration U.S. (2003), “Progressive collapse analysis and design guidelines for new federal office buildings and major modernization projects”, Washington (DC).
- Hoang V.L., Jaspart J.P. and Demonceau J.F.(2015), “Extended end-plate to concrete-filled rectangular column joint using long bolts”, *J. Constr. Steel Res.*, **113**: 156-168.
- Hoffman S.T. and Fahnestock L.A. (2011), “Behavior of multi-story steel buildings under dynamic column loss scenarios”, *Steel and Composite Structures*, **11**(2): 149-168.
- Huang Z., Jiang L.Z., Zhou W.B. and Chen S. (2016), “Studies on restoring force model of concrete filled steel tubular lace column to composite box-beam connections”, *Steel and Composite Structures*, **22**(6): 1217-1238.
- Izzuddin B.A., Vlassis A.G., Elghazouli A.Y. and Nethercot D.A. (2008), “Progressive collapse of multi-storey buildings due to sudden column loss-Part 1: Simplified assessment framework”, *Engineering Structures*, **30**(5): 1308-1318.
- Li W., Han L.H. (2011), “Seismic performance of CFST column to steel beam joints with RC slab: Analysis”, *J. Constr. Steel Res.*, **67**(1): 127-139.
- Khaloo A. and Omidi H. (2018), “Evaluation of vierendeel peripheral frame as supporting structural element for prevention of progressive collapse”, *Steel and Composite Structures*, **26**(5): 549-556.
- Mashhadi J. and Saffari H. (2017), “Dynamic increase factor based on residual strength to assess progressive collapse”, *Steel and Composite Structures*, **25**(5): 617-624.
- Mirtaheeri M. and Zoghi M.A. (2016), “Design guides to resist progressive collapse for steel structures”, *Steel and Composite Structures*, **20**(2): 357-378.
- Tartaglia R., D’Aniello M. Zimbru M. and Landolfo R. (2018), “Finite element simulations on the ultimate response of extended stiffened end-plate joints”, *Steel and Composite Structures*, **27**(6): 727-745.
- Simoes da Silva L., Lima L.R.O., Vellasco P.C.G. and Andrade S.A.L. (2004), “Behaviour of flush end-plate beam-to-column joints under bending and axial force”, *Steel & Composite Structure*, **4**(2):77-94.
- Sadek F., Main J.A., Lew H.S. and Bao Y.H. (2011), “Testing and analysis of steel and concrete beam-column assemblies under a column removal scenario”, *Journal of Structural Engineering*, **9**: 881-892.
- Stylianidis P.M. and Nethercot D.A. (2015), “Modelling of connection behaviour for progressive collapse analysis”, *J. Constr. Steel Res.*, **113**:169-184.
- Thai H.T. and Uy B.(2016), “Rotational stiffness and moment resistance of bolted endplate joints with hollow or CFST columns”, *J. Constr. Steel Res.*, **126**: 139-152.
- Xu M, Gao S, Zhang S, Li H. (2018), “Experimental study on bolted CFST-column joints with different configurations in accommodating column-loss”, *J. Constr. Steel Res.*, **151**: 122-131.
- Wang J.F., Chen L.P. (2012), “Experimental investigation of extended end plate joints to concrete-filled steel tubular columns”, *J. Constr. Steel Res.*, **79**: 56-70.
- Yang B. and Tan K.H. (2012), “Numeirical analyses of steel beam-column joints subjected to catenary action”, *J. Constr. Steel Res.*, **70**: 1-11.